Plant Physiology and Biochemistry 138 (2019) 130–139

Contents lists available at ScienceDirect

Plant Physiology and Biochemistry

journal homepage: www.elsevier.com/locate/plaphy

Research article

Transcriptome and chemical analysis reveal putative genes involved in flower color change in *Paeonia* 'Coral Sunset'

Liping Guo[a,b,1], Yujiao Wang[a,b,1], Jaime A. Teixeira da Silva[c], Yongming Fan[a,b], Xiaonan Yu[a,b,*]

[a] School of Landscape Architecture, Beijing Forestry University, Beijing, 100083, PR China
[b] Beijing Key Laboratory of Ornamental Plants Germplasm Innovation & Molecular Breeding, National Engineering Research Center for Floriculture, Beijing Laboratory of Urban and Rural Ecological Environment, Beijing, 100083, PR China
[c] P. O. Box 7, Miki–cho Post Office, Ikenobe 3011–2, Kagawa–ken, 761-0799, Japan

ARTICLE INFO

Keywords:
Anthocyanin
Flavonoid
Flower color
Gene expression and regulation
Transcriptome

ABSTRACT

The flower color of *Paeonia* 'Coral Sunset' and 'Pink Hawaiian Coral' changes from coral to pink to pale yellow during flowering, which confers high ornamental value to these two cultivars. However, the molecular mechanism underlying flower color change is still unclear. In this study, flavonoids in petals of *Paeonia* 'Coral Sunset' and 'Pink Hawaiian Coral' at seven flowering stages were analyzed to explore the effects of the flavonoid component on changes in flower color. In addition, four cDNA libraries of 'Coral Sunset' during the critical blooming stages were constructed and the transcriptome was sequenced to investigate the molecular mechanism underlying changes to flower color. Two anthocyanins (cyanidin-3,5-di-*O*-glucoside and peonidin-3,5-di-*O*-glucoside) were detected in both cultivars. Total anthocyanin content in both cultivars accumulated continuously from stages 1–3 and then decreased sharply. Correlation analysis showed that the change in flower color from coral to pink to pale yellow is due to a significant decrease in anthocyanin content. A total of 91,583 Unigenes were obtained in 'Coral Sunset', 33,962 (37.08%) of which were annotated to major databases. Based on the enrichment analysis of differentially expressed genes, eight structural genes (*CHS*, *F3H*, *F3'H*, *FLS*, *DRF*, *ANS*, *ANR* and *UFGT*) and 13 transcription factors (five *MYB*, three *bHLH*, one *WD40*, one *HY5*, one *PIF3*, one *COP1* and two *PHY*) related to flavonoid biosynthesis were screened. The qRT-PCR results were generally consistent with the high-throughput sequencing results. This research will provide a foundation to clarify the mechanisms underlying changes in flower color of herbaceous peony.

1. Introduction

Herbaceous peony (*Paeonia lactiflora* Pall.), which belongs to the *Paeoniaceae* family, is a famous traditional flower in China and is widely used in landscaping and as a cut flower (Yu et al., 2010). It is a symbol of wealth and honor in Chinese culture (Zhao et al., 2017). Herbaceous peony cultivars are rich in color and have been categorized into nine groups: white, pink, red, purple, black, blue, yellow, green and double colors (Wang and Zhang, 2005). Interestingly, some cultivars change flower color during flowering, such as 'Coral Sunset' and 'Pink Hawaiian Coral'. The colors of 'Coral Sunset' and 'Pink Hawaiian Coral' flowers change from coral to pink to pale yellow during flowering. This characteristic confers high ornamental and research value to these two cultivars. Many plants have the attribute of changing flower color during flowering. The color of *Victoria amazonica* and *Victoria cruziana* flowers is white on the first blooming night but then changes into pink or ruby during the second blooming night (Wu et al., 2018). Petals of *Oenothera tetraptera* change from white to pink while those of *Oenothera laciniata* change from yellow to orange during senescence (Teppabut et al., 2018).

Flower color, an important ornamental trait of plants, can be affected by pigments, cell sap pH, and metal ions. Among these, the pigment component is the most important factor. There are three major classes of flower pigments: flavonoids, betalains, and carotenoids (Tanaka et al., 2009). Among the flavonoids, anthocyanins provide a wide range of colors ranging from orange to blue while flavones and flavonols are mainly related to yellow color in petals and also function as co-pigments (Xue et al., 2016). Research on flower coloration and pigments of herbaceous peony has made great progress. Jia et al. (2008) detected five major anthocyanins (peonidin-3,5-di-*O*-glucoside (Pn3G5G), pelargonidin-3,5-di-*O*-glucoside (Pg3G5G), cyanidin-3,5-di-*O*-glucoside (Cy3G5G), peonidin-3-*O*-glucoside (Pn3G), and cyanidin-3-

* Corresponding author. No.35, Tsinghua East Road, Haidian District, Beijing, 10083, PR China.
E-mail address: yuxiaonan626@126.com (X. Yu).
[1] These authors contributed equally to this work.

https://doi.org/10.1016/j.plaphy.2019.02.025
Received 27 December 2018; Received in revised form 15 February 2019; Accepted 27 February 2019
Available online 04 March 2019
0981-9428/

O-glucoside (Cy3G)) in 41 herbaceous peony cultivars. Zhao et al. (2016) reported that Pn3G5G may be the dominant anthocyanin in red herbaceous peony 'Dahonglou' flowers. In addition, the flavonoid biosynthetic pathway has been studied in detail. In the flavonoid metabolic pathway, the expression of upstream genes such as *CHS*, *CHI*, *F3H* and *FLS* contribute to the synthesis of flavones/flavonols, while downstream genes such as *DRF*, *ANS* and *GT* promote the synthesis of anthocyanins (Zhao et al., 2012, 2014). Zhao et al. (2016) found that *PlDRF* and *PlANS* play a key role in anthocyanin biosynthesis and contribute to pink and red coloration of herbaceous peony petals.

However, the mechanism underlying color change in herbaceous peony during flowering is still unclear. To investigate the mechanism, two promising cultivars 'Coral Sunset' and 'Pink Hawaiian Coral', which change flower color during flowering, were selected as experimental materials. In this study, we identified flavonoids in petals from seven stages via high performance liquid chromatography (HPLC) and analyzed the relationship between flower coloration and pigment content. Furthermore, comparative transcriptomic analysis of four critical stages of flowering in 'Coral Sunset' was conducted to identified the differentially expressed genes (DEGs) related to flavonoid biosynthesis. This research would be helpful to elucidate the mechanism of flower color change in herbaceous peony.

2. Material and methods

2.1. Plant materials

Petals of 'Coral Sunset' and 'Pink Hawaiian Coral' were used as experimental materials. Samples were collected at seven different flowering stages (0 h, 24 h, 48 h, 72 h, 96 h, 120 h and 144 h) (Fig. 1) during May 2016 at Xiaotangshan experimental nursery, Beijing Forestry University, Beijing, China. A spectrophotometer (NF555, Nippon Denshoku Industries Co. Ltd., Japan) was used to measure the color-related value of L^*, a^*, b^*, C^* and h of fresh petals. Materials for other tests were placed in liquid nitrogen immediately and stored at −80°C.

2.2. Extraction and qualitative and quantitative analysis of flavonoids

Freeze-dried petals were ground in liquid nitrogen and powder (0.2 g) of each sample was extracted with a reagent (methanol: water: formic acid: trifluoroacetic acid = 70:27:2:1, v/v), then ultrasonicated for 30 min at 20 °C. Extracts were centrifuged at 12000 rpm for 20 min and the supernatants were collected. This procedure was repeated twice. All supernatants were combined and filtered through a 0.22 μm nylon membrane filter (Shanghai ANPEL Scientific Instruments, Shanghai, China). Three biological replicates were prepared for each sample.

Chromatographic analysis was carried out with an HPLC (Waters-2695, the USA) equipped with a 996PDA detector. The HPLC column was WondaCr act ODS-2 C18 (4.6 mm × 250 mm, Shimadzu, Kyoto, Japan). The chromatographic conditions are detailed in Deng et al. (2015). Total spectral wavelength ranged from 200 to 600 nm. The detection wavelength of anthocyanins and flavones/flavonols was 520 nm and 350 nm, respectively. Flavonoid content was calculated using a semi-quantitative method (Zhong et al., 2012). Cy3G5G and quercetin-3-*O*-rutinoside (rutin) were the respective standards used to calculate the content of TA (total anthocyanins) and TF (total flavones/flavonols). A qualitative flavonoid analysis was carried out with an HPLC-ESI-MS (Waters-2795 HPLC/MS Q-TOF, Milford, MA, USA). Total ion scanning mass (m/z) range was 50–1000 u, capillary voltage was 4500 V, atomization pressure was 35 psi, dry gas (N_2) temperature was +180°C and gas velocity was 8.0 L/min.

Furthermore, to investigate the relationship between flower color and flavonoid components, multiple linear regression (MLR) was established by SPSS version19.0. The contents of TA and TF were independent variables, and the L^*, a^*, and b^* values were dependent variables. CI (co-pigment index, TF/TA) was used to evaluate co-pigment effect between anthocyanins and flavones/flavonols on floral coloration.

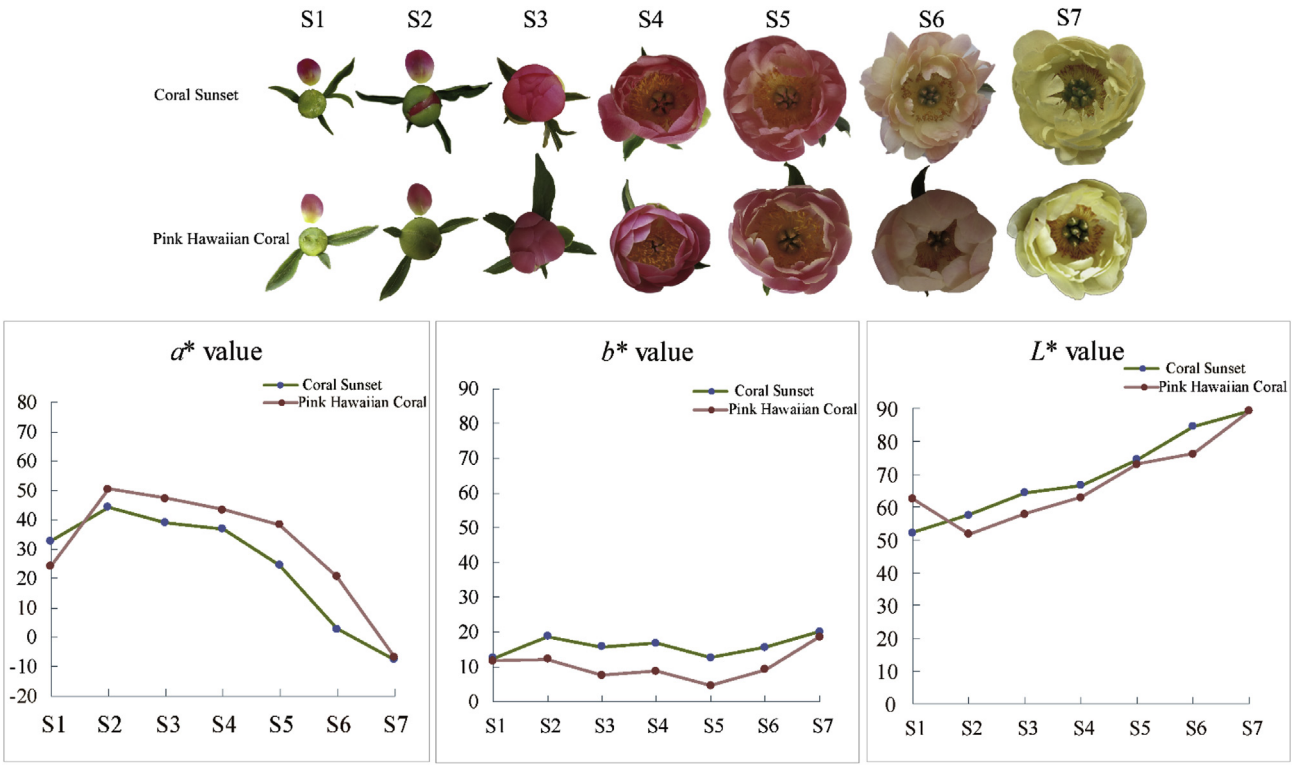

Fig. 1. Different developmental stage and chroma values of flowers of peony 'Coral Sunset' and 'Pink Hawaiian Coral' in seven developmental stages. (For interpretation of the references to color in this figure legend, the reader is referred to the Web version of this article.)

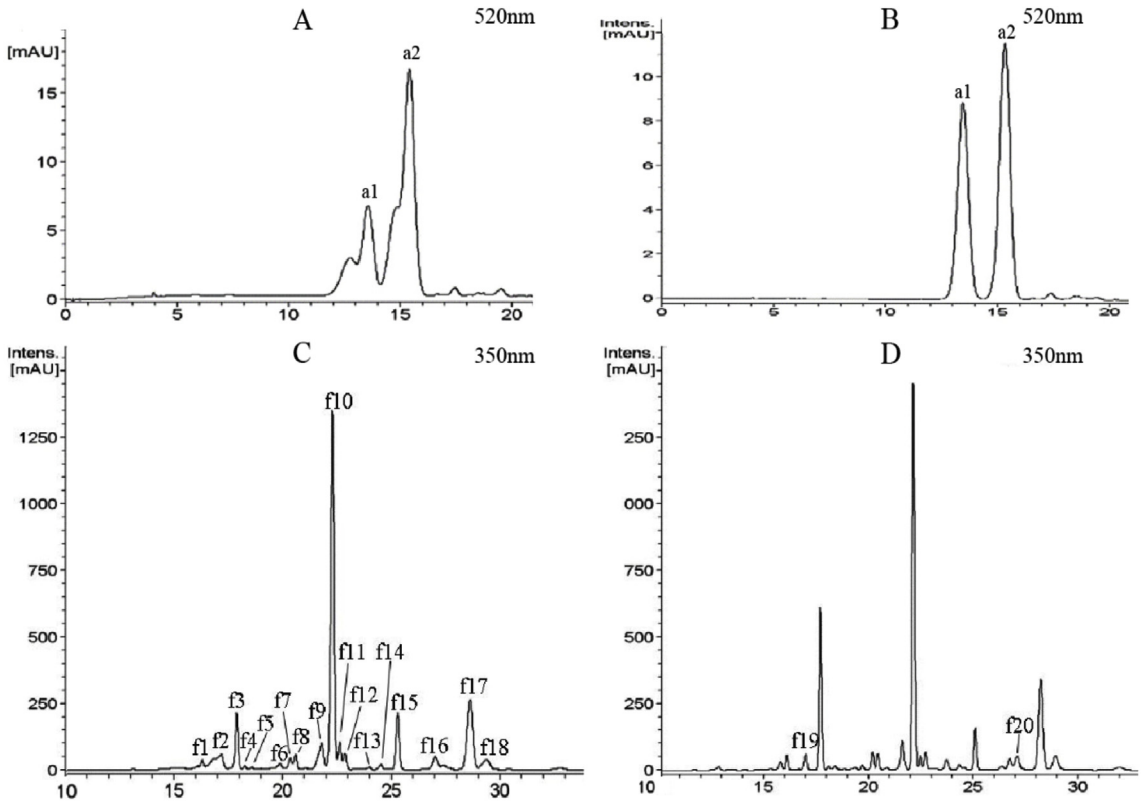

Fig. 2. HPLC chromatograms of flavonoids detected at 520 and 350 nm in 'Coral Sunset' and 'Pink Hawaiian Coral'. A: Anthocyanins detected in Paeonia 'Coral Sunset'; B: Anthocyanins detected in 'Pink Hawaiian Coral'; C: Flavones/flavonols detected in 'Coral Sunset'; D: Flavones/flavonols detected in 'Pink Hawaiian Coral'.

2.3. RNA extraction, cDNA library construction and transcriptome sequencing

Total RNA was extracted using a plant total RNA rapid extraction kit (Omega Total RNA Kit II) (OMEGA, Norcross, GA, USA) according to the manufacturer's instructions. The concentration and purity of total RNA was validated with a Nanodrop ND-100 spectrophotometer (NanoDrop Technologies; DE, USA) and Agilent 2100 Bioanalyzer (Agilent Technologies, CA, USA) and its integrity was verified by agarose gel electrophoresis. After RNA samples were validated, RNA-seq libraries were prepared and sequenced at Biomarker Technologies (Beijing, China). Transcriptome sequencing was conducted on the Illumina HiSeq X-ten high throughput sequencing platform. Three biological replicates were prepared for each sample.

2.4. De novo assembly and annotation

Raw reads were filtered by removing adaptor sequences and low-quality sequences to obtain high-quality reads. The high-quality reads were assembled *de novo* by the Trinity program (Grabherr et al., 2011) and the longest transcripts were selected as the Unigenes. Functional annotation was performed by aligning Unigenes with following databases: NR (NCBI non-redundant protein sequences), Pfam (Protein family), COG (Clusters of Orthologous Groups of proteins), Swiss-Prot (a manually annotated and reviewed protein sequence database), KEGG (Kyoto Encyclopedia of Genes and Genomes) and GO (Gene Ontology).

2.5. Identification and analysis of DEGs

Clean reads were aligned to Unigenes and expression level was calculated by the FPKM (Fragments Per Kilobase of transcriptome per Million mapped reads) method (Mortazavi et al., 2008). DEGs were identified using the DESeq R package (Anders and Huber, 2010) based on FDR < 0.01 and FC ≥ 2 and then subjected to GO classification enrichment and KEGG enrichment analysis. Based on enrichment, DEGs involved in flavonoid biosynthesis were screened and subjected to protein-protein interaction analysis using the online program STRING (http://string-db.org/cgi/input.pl) to further analyze the regulatory network of these genes.

2.6. RT-qPCR analysis of putative DEGs

The expression of key genes in petals of 'Coral Sunset' were measured using RT-qPCR. A 25 μl reaction system was formulated based on the instructions of TB Green TaKaRa Premix Ex Taq™ II (Tli RNaseH Plus; TaKaRa Bio Inc., Japan). Amplification proceeded as follows: predenaturation at 95 °C for 30 s, 40 cycles at 95 °C for 5 s, annealing for 30 s and 72 °C for 30 s. Dissolution curves were recorded from 65 °C to 95 °C with a 0.5 °C increase every 5 s. Each reaction was repeated three times. Relative expression level of target genes was calculated by $2^{-\Delta\Delta Cq}$ and relevant data were analyzed by SPSS version19.0 software and Origin 8 software.

3. Results

3.1. Floral color phenotype

The colors of 'Coral Sunset' and 'Pink Hawaiian Coral' flowers changed across seven flowering stages (Fig. 1A) and the chroma values of these two cultivars was close and the change in trend was similar (Fig. 1B; Supplementary file 1, Table S1). The a^* value, which represents redness, increased from S1 to S2 and then kept declining from S2 to S7. In 'Coral Sunset' petals, it increased from 32.92 (S1) to 44.27 (S2) and then declined to −7.47 (S7). In petals of 'Pink Hawaiian Coral', it changed from 24.35 (S1) to 50.45 (S2) and then declined to −6.68 (S7). The b^* value of these two cultivars, which represents

Table 1
Chromatographic and spectral data of anthocyanins from 'Coral Sunset' and 'Pink Hawaiian Coral'.

Peaks	Retention time (min)	λ_{max}(nm)	ESI-(+)-MS(m/z)	Tentative identification
a1	13.5	277.3/519.9	611.2, 449.1, 287.1	Cyanidin-3,5-di-O-glucoside
a2	15.4	280.9/513.8	625.2, 463.1, 301.2	Peonidin-3,5-di-O-glucoside
f1	16.3	254, 321	627[M+H]+, 465[M+H-162]+, 303[Y0+]	Quercetin-3,7-di-O-glucoside
f2	16.8	253, 350	611[M+H]+, 499[M+H-162]+, 287[Y0+]	Luteolin-3,7-di-O-glucoside
f3	17.9	265, 347	611[M+H]+, 499[M+H-162]+, 287[Y0+]	Kaempferol-3,7-di-O-glucoside
f4	18.3	251, 353	641[M+H+Na]+, 303[Y0+]	Quercetin -7-O-galloylglucoside
f5	18.6	233, 332	641[M+H+Na]+, 303[Y0+]	Quercetin -3-O-galloylglucoside
f6	19.9	236, 342	643[M+H]+, 481[M+H-162], 319[Y0+]	Myricetin −3,7-di-O-glucoside
f7	20.3	216, 276	611[M+H]+, 305	Unknown
f8	20.6	253, 353	611[M+H]+, 449[M+H-162]+, 303[Y0+]	Quercetin-3-rhamnoside -7- glucoside
f9	21.8	275, 326	619[M+H+Na]+, 465[M+H+Na-132], 303[Y0+]	Quercetin -3-glucoside-7- arabinoside
f10	22.3	264, 347	595[M+H]+, 433[M-162]+, 287[Y0+]	Kaempferol-3-hamnoside-7- glucoside
f11	22.6	253, 354	619[M+H]+, 305	Unknown
f12	22.9	265, 349	619[M+H+Na]+, 287[Y0+]	Kaempferol-3-glucoside-7-rhamnoside
f13	24	244, 357	597[M+H]+, 435[M-162]+, 303[Y0+]	Quercetin-3-arabinoside-7-glucoside
f14	24.5	217, 278	619, 303	Unknown
f15	25.3	254, 354	465[M]+, 303[Y0+]	Quercetin-3-O-glucoside
f16	27	270, 321	479[M+H]+, 317[Y0+]	Isorhamnetin-3-O-glucoside or Isorhamnetin -7-O-glucoside
f17	28.6	265, 348	449[M+H]+, 287[Y0+]	Kaempferol-3-O-glucoside
f18	29.4	263, 366	449[M+H]+,287[Y0+]	Kaempferol-7-O-glucoside
f19	17	217, 275	303	Unknown
f20	27.1	241, 348	601[M+H]+, 287[Y0+]	Luteolin-3-O-galloylglucoside or Luteolin-7-O-galloylglucoside

blueness, fluctuated throughout flowering and was higher during S7 (20.10 in 'Coral Sunset' and 18.63 in 'Pink Hawaiian Coral') than in other stages. The L^* value, which represents lightness, increased consistently in 'Coral Sunset' throughout the seven flowering stages, from 52.20 (S1) to 89.42 (S7) but first decreased from 62.5 (S1) to 51.86 (S2) and then increased from 51.86 (S2) to 89.43 (S7) in 'Pink Hawaiian Coral' petals.

3.2. Qualitative and quantitative analysis of anthocyanins

Two peaks of anthocyanin (a1 and a2) were detected in both cultivars while 18 and 20 flavones/flavonols were detected in 'Coral Sunset' and 'Pink Hawaiian Coral' respectively (Fig. 2). Anthocyanins and flavones/flavonols were identified by comparison with HPLC retention time, elution order, UV–vis spectrum and MS fragmentation pattern in published data (Table 1). The UV–vis spectrum of peak a1 (519.9) and peak a2 (513.8) indicated that a1 was a cyanidin-based anthocyanin and a2 was a peonidin-based anthocyanin. Peaks a1 and peak a2 were further confirmed by their mass spectra. The mass to charge ratio (m/z) of a1 was 611 u, 449 u and 287 u and its specific m/z was 287 u, so it was identified as cyanidin. The difference between m/z 611 to m/z 449 and m/z 449 to m/z 287 was 162 u, which indicated that a1 was a cyanidin derivative with two glucosides. The third and fifth hydroxyl groups of anthocyanidin are most susceptible to glycosylation (Constant et al., 2015). Therefore, a1 was tentatively established as cyanidin-3,5-di-O-glucoside. The m/z of a2 was 625 u, 463 u, and 301 u and the specific m/z was 301, so it was identified as peonidin. Similarly, a2 was tentatively established as peonidin-3,5-di-O-glucoside. In addition, four kinds of flavonol were identified: luteolin (f2, f20), quercetin (f1, f4, f5, f8, f9 and f15), kaempferol (f3, f10 and f12) and myricetin (f6).

The flavonoid content varied significantly across different stages of flowering (Supplementary file 1.Table S2). Just like chroma values, the TA of both cultivars changed in a similar manner (Fig. 3): it increased rapidly from S1 to S3 and then declined sharply and was almost undetectable at S7 (2.5 μg/g in 'Coral Sunset' and 1.6 μg/g in 'Pink Hawaiian Coral'). The trend of TF in both cultivars was also similar: it increased significantly from S1 (2867 μg/g in 'Coral Sunset' and 1208 μg/g in 'Pink Hawaiian Coral') to S2 (5582 μg/g in 'Coral Sunset' and 4464 μg/g in 'Pink Hawaiian Coral'), then decreased, increasing slightly in the final stage. CI presented a sharp rise from S6 (287 in 'Coral Sunset' and 118 in 'Pink Hawaiian Coral') to S7 (1886 in 'Coral Sunset' and 2465 in 'Pink Hawaiian Coral').

The relationship between flower color and flavonoid components was analyzed by MLR and two equations were obtained:

$L^* = 55.406–0.122\ TA + 0.007\ TF\ (R^2 = 0.756)$;

$a^* = 27.507 + 1.73\ TA – 0.005\ TF\ (R2 = 0.689)$

These two equations indicate that the L^* and a^* values were correlated with TA and TF, especially with TA. TF had a positive effecte on the L^* value and a negative effect on the a^* value. TA had a negative effect on the L^* value but a positive effect on the a^* value. In contrast, there was no strong correlation between the b^* value and TA or TF, which indicates that the yellow or blue color in 'Coral Sunset' and 'Pink Hawaiian Coral' was influenced by other factors.

3.3. Overview of transcriptome sequencing

RNA-seq sequencing of four critical blooming stages (S1, S3, S5 and S7) of 'Coral Sunset' was performed and 32.02 Gb of clean reads were obtained with a Q30 value of 94.77% and a GC content of 44.5–44.7% (Table 2), which indicated that the overall sequencing was of high quality. Based on clean reads, 91583 Unigenes were assembled with an average length of 721.89 bp and an N50 of 1123 bp (Table 3 and Supplementary file 2).

3.4. Functional annotation of Unigenes

In total, 33962 Unigenes were annotated, accounting for 37.08% of total Unigenes (Table 4). Among them, 33,445 (36.52%), 21,217 (23.17%), and 20,851 (22.77%) Unigenes could be annotated to NR, Swiss-Prot and Pfam databases, respectively. In the COG database, only 9167 Unigenes were annotated, accounting for 10.01% of the total.

3.5. Analysis of DEGs identified in the four libraries

Analysis of DEGs was performed between every two sequential stages (S1/S3, S3/S5, and S5/S7) based on FPKM with thresholds FDR < 0.01 and FC > 2 and 1418 DEGs (678 up- and 740 down-regulated) between S1 and S3 libraries, 695 DEGs (390 up- and 305 down-regulated) between S3 and S5 libraries, and 618 DEGs (330 up- and 288 down-regulated) between S3 and S5 libraries were identified (Fig. 4A). In total, there were 1329 up- regulated and 1298 down-

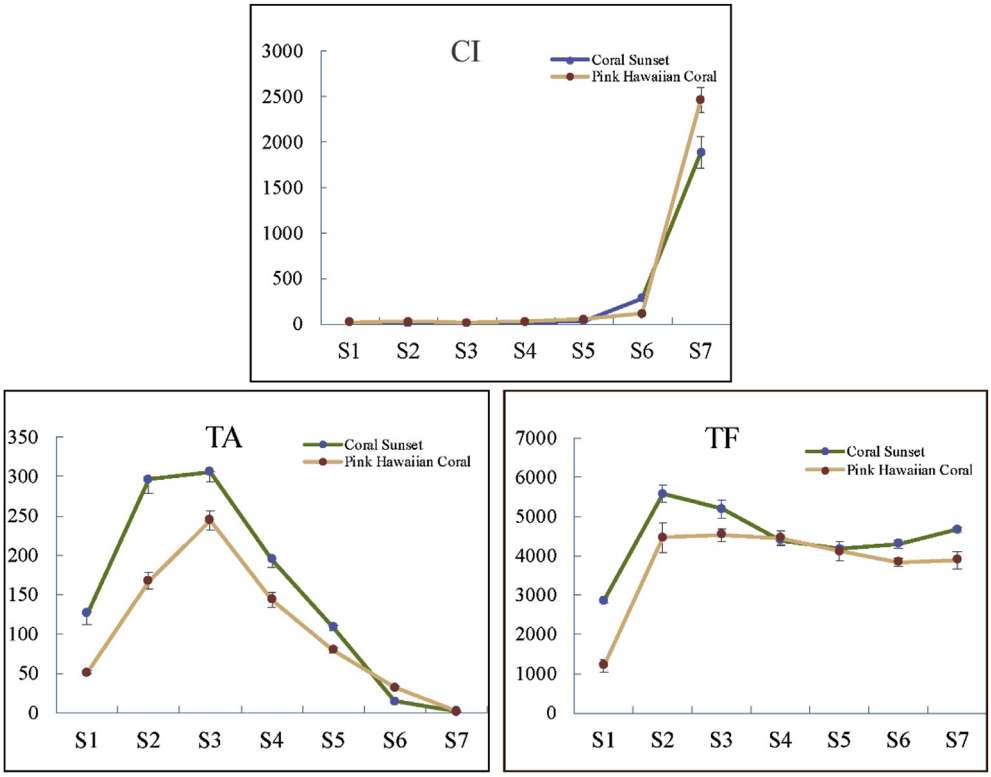

Fig. 3. Total content of anthocyanins (TA), flavones/flavonols (TF) and co-pigment index (CI) in petals of 'Coral Sunset' than 'Pink Hawaiian Coral' during seven stages of flowering. (For interpretation of the references to color in this figure legend, the reader is referred to the Web version of this article.)

Table 2
Data quality statistics of RNA-seq in *Paeonia* 'Coral Sunset' petals.

Libraries	Total raw reads	Clean reads	GC (%)	N (%)	Q20%
S1	27,411,111	27,194,563	44.78%	0.01%	97.84%
S3	29,139,835	28,880,490	44.54%	0.01%	97.81%
S5	26,010,927	25,808,042	44.60%	0.01%	97.76%
S7	25,359,718	25,151,768	44.57%	0.01%	97.90%

Table 3
Summary for the transcriptome assembly of *Paeonia* 'Coral Sunset'.

Assembly	Total number	Total length	N50 length	Average length
Transcripts	179,087	158,485,986	1316	884.97
Unigenes	91,583	66,113,042	1123	721.89

Table 4
Annotation of Unigenes against public databases.

Database	Annotated number	Relative %
COG	9167	10.01%
GO	20129	21.98%
KEGG	12163	13.28%
Pfam	20851	22.77%
Swiss-prot	21217	23.17%
NR	33445	36.52%
All annotated	33962	37.08%

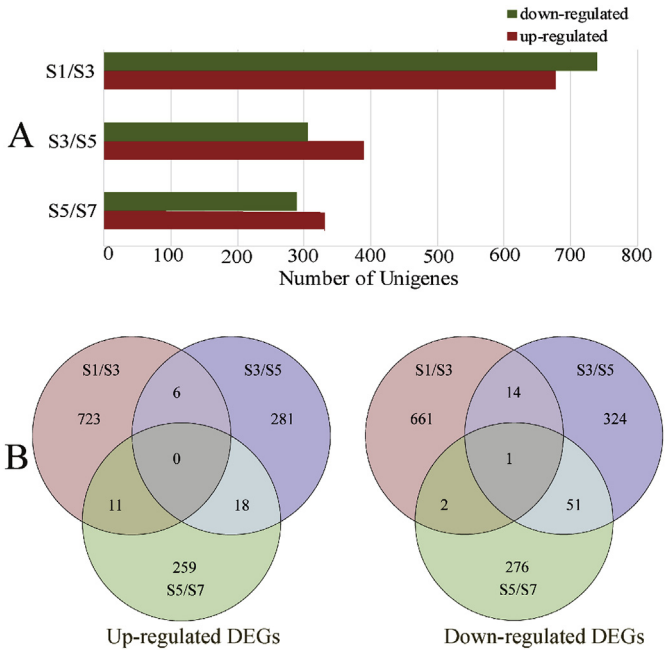

Fig. 4. A: Up-regulated and down-regulated DEGs between sequential stages. B: Venn diagram of total up-regulated and down-regulated DEGs.

regulated DEGs among the three comparison groups (Fig. 4B).

A total of 481 up-regulated DEGs and 179 down-regulated DEGs were enriched into GO terms. The main terms were "catalytic activity", "metabolic process", "cell", "single-organism process" and "binding" (Fig. 5). A total of 143 up-regulated DEGs and 179 down-regulated DEGs were enriched into KEGG pathways and the main pathways were "Protein processing in endoplasmic reticulum" (ko04141), "Plant hormone signal transduction" (ko04075), and "Phenylpropanoid biosynthesis" (ko00940) (Fig. 5). Three enriched pathways were related to flavonoid biosynthesis including "flavonoid biosynthesis" (k00941), "flavone and flavonol" (k00944), and "anthocyanin biosynthesis" (k00942). Unigenes enriched to pathways related to flavonoid biosynthesis were mainly down-regulated.

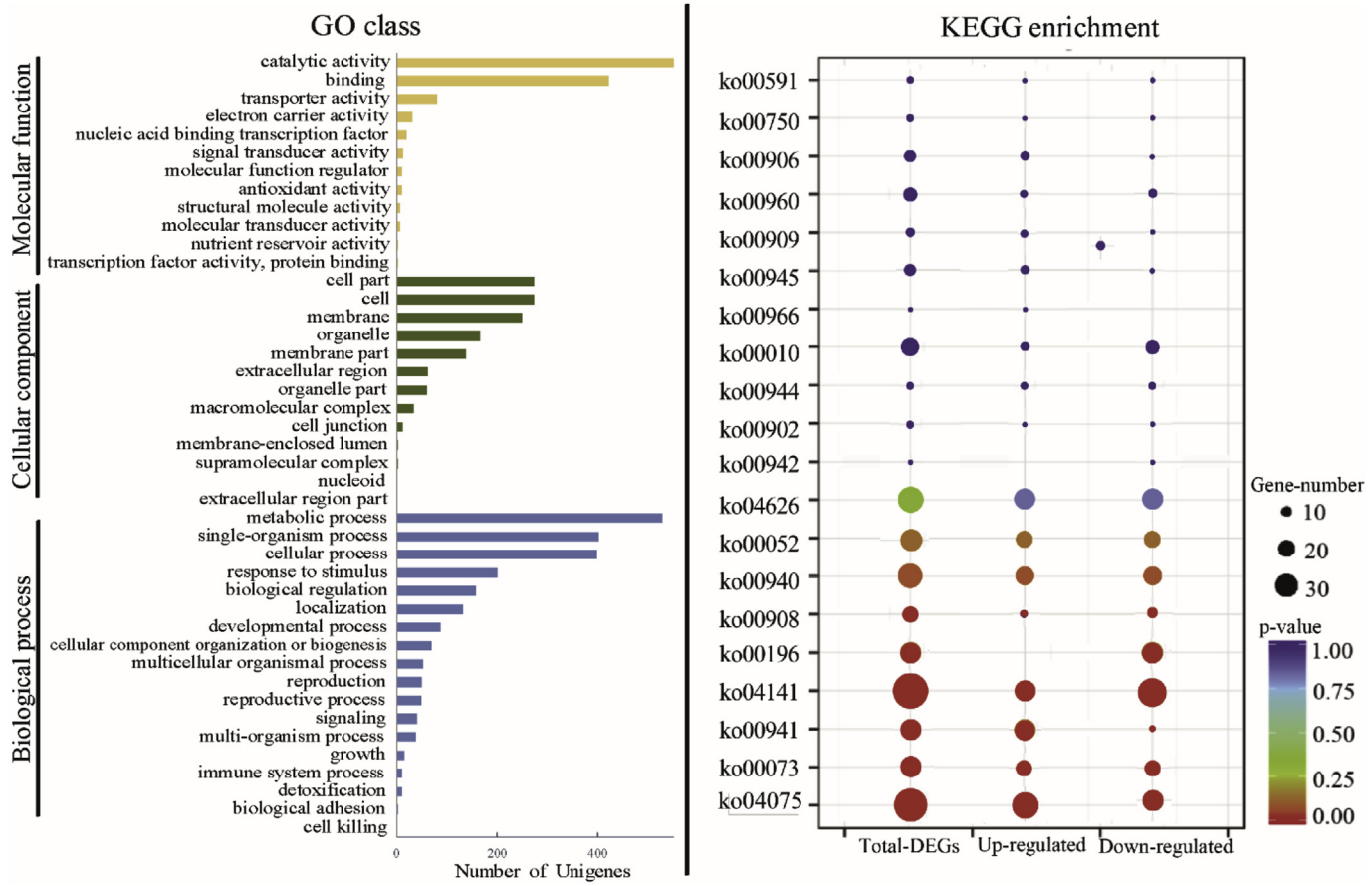

Fig. 5. GO enrichment and KEGG enrichment of DEGs.

3.6. Identification of structural genes involved in the flavonoid biosynthetic pathway

Based on functional annotation, as well as GO enrichment and KEGG enrichment of DEGs, eight structural genes that might play a key role in floral color changes in 'Coral Sunset' were screened (Fig. 6 and Table 5), including *PlCHS* (c107467.graph_c0), *PlF3H* (c108658.graph_c0), *PlF3′H* (c117094.graph_c0), *PlFLS* (c97130.graph_c0), *PlDRF* (c110625.graph_c0), *PlANR* (c43422.graph_c0), *PlANS* (106996.graph_c0) and *PlUFGT* (108735.graph_c0).

The RPKM values of these eight genes diaplayed a significant difference across different stages. All these genes shared a similar expression pattern: displaying the highest levels and then decreasing sharply. During S7, the expression of these genes was almost undetectable. The high level of these genes during S1 could contribute to the accumulation of anthocyanins from S1 to S3, leading to an increase of the a^* value and a decrease of the L^* value. The significantly decreasing expression of these structural genes from S3 to S7 resulted in the reduction of anthocyanin, leading to an increase of the L^* value and a decrease of the a^* value.

3.7. Identification of transcription factors

Based on GO and KEGG enrichment, transcription factors (TFs) coded for by DEGs and eight structural genes were subjected to protein-protein interaction analysis to screen critical TFs regulating anthocyanin synthesis. A protein-protein interaction network showed that eight *R2R3-MYB*, six *bHLH*, one *WD40*, one *HY5* (*ELONGATED HYPOCOTYL 5*), one *PIF3* (*PHYTOCHROME INTERACTING FACTOR 3*), one *COP1* (*CONSTITUTIVE PHOTOMORPHOGENIC 1*) and two *PHY* (Phytochrome A and Phytochrome B) TFs (Fig. 7 and Table 6) might participate in the regulation of the eight structural genes (Fig. 7A). As shown in the diagram, these structural genes might be regulated by other TFs through HY5. In addition, co-expression between TFs and structural genes was analyzed using SPSS version 19 by calculating Pearson's coefficient of their FPKM. Strong correlations were observed between the 13 TFs and the eight structural genes (Fig. 7B). *bHLH78*, *MYB17*, *MYB59*, *MYB61* and *WD40* were strongly and positively correlated with the structural genes while *bHLH-a*, *bHLH128*, *MYB73*, *MYB82*, *PIF3*, *PHYB*, *HY5* and *COP1* had strong negative correlations with structural genes.

Based on an interaction network and co-expression between TFs and structural genes, a model describing the regulation is proposed in Fig. 8. PIF3 and *COP1*, which were positively regulated by *PHYB*, could positively regulate the expression of *HY5*. The expression of *HY5* could also be positively regulated by TFs *MYB82*, *bHLH-a* and *bHLH128* and negatively regulated by TFs *bHLH78*, *MYB17*, *MYB83* and *WD40*. *HY5*, together with *MYB61*, could regulate the expression of the structural genes.

3.8. Validation of anthocyanin biosynthesis structural genes

To confirm the accuracy of the RNA-seq results, six structural genes in the flavonoid metabolic pathway were selected to analyze the relative expression level of 'Coral Sunset' during seven blooming stages by qRT-PCR (Fig. 9). Pearson's correlation coefficient was used to determine the correlation between RNA-seq results and qRT-PCR of the same stages (S1, S3, S5, S7). The correlation coefficient between log2 (FPKM) by RNA-seq and log2 ($2^{-\Delta\Delta Cq}$) by qRT-PCR was 0.755 (Fig. 7), which indicates that the RNA-seq data were credible and reliable.

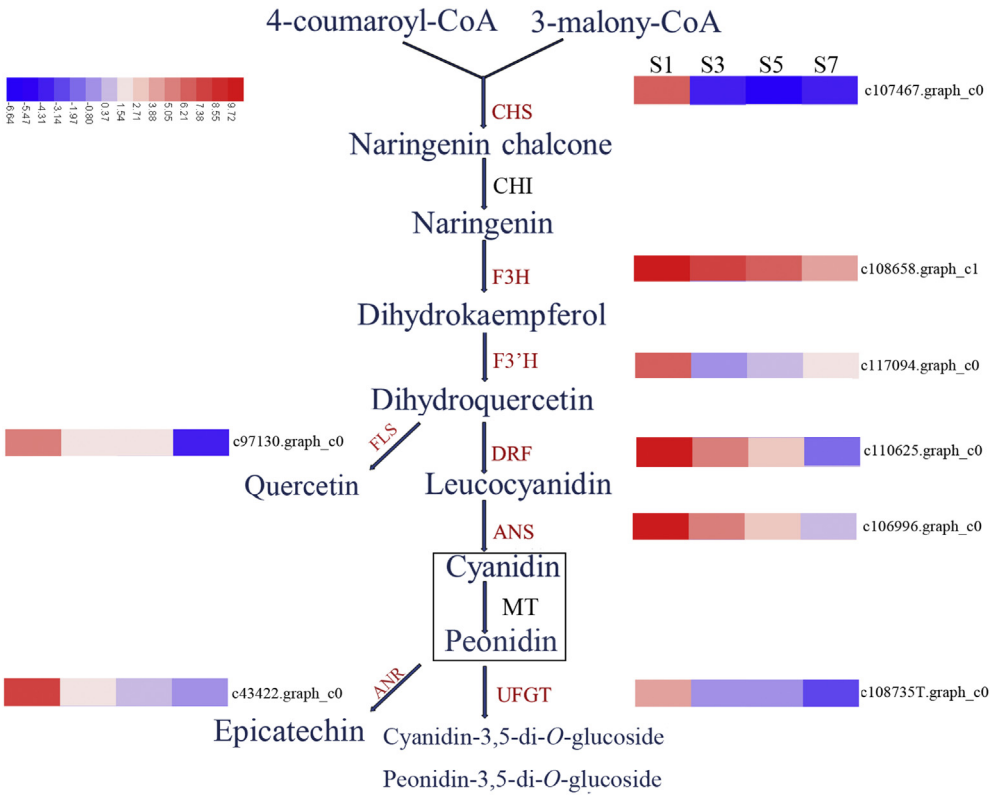

Fig. 6. Putative genes in the anthocyanin synthesis pathway and their expression level. Heatmaps were constructed based on log2 (RPKM) of petals during S1, S3, S5 and S7.

Table 5
FPKM of key anthocyanin biosynthesis related genes in petals of peony 'Coral Sunset' during different stages of flowering.

Gene name	#ID	Expression profile (FPKM)			
		S1	S3	S5	S7
PlCHS	c107467.graph_c0	135.02	0.08	0.01	0.09
PlF3H	c108658.graph_c1	1897.75	255.56	81.07	16.01
PlF3'H	c117094.graph_c0	131.04	0.67	2.84	4.96
PlFLS	c97130.graph_c0	35.89	4.23	3.46	0.11
PlANR	c43422.graph_c0	221.38	3.01	1.32	1.27
PlUFGT	c108735.graph_c0	27.86	0.98	1.04	0.23
PlDFR	c110625.graph_c0	1194.54	70.49	12.35	0.53
PlANS	c106996.graph_c0	1381.94	57.95	11.36	1.37

4. Discussion

The color of peony flowers is related to the composition and content of flavonoids, such as anthocyanin, flavones and flavonols. There are seven common anthocyanidins in nature: pelargonidin (Pg), cyanidin (Cy), delphinidin (Dp), peonidin (Pn), petunidin (Pt), malvidin (Mv) and primulagenin (Pm), and among them Cy and Pn are responsible for red color (Liu et al., 2016). Flavones and flavonols play an important role in yellow coloration (Xue et al., 2016). The phenomenon of changing colors characterizes many ornamental plants, such as *Lonicera japonica*, *Brunfelsia acuminate* and *Brunfelsia calycina* (Cao, 2012; Fu et al., 2013; Zipor et al., 2015). This phenomenon has very high ornamental and research value. However, research on the mechanism of changing colors is very limited, including in peony.

In this study, we detected the component of anthocyanins and flavones/flavonols to explore the mechanism of changing flower color in in two cultivars of peony, 'Coral Sunset' and 'Pink Hawaiian Coral'. The resulted indicated that flower color change was related to TA and TF content, especially TA content. The reduction of anthocyanins resulted in an increase of L^* value and a decrease of a^* value, which was the main reason for the transformation from coral to pink to yellow. Our findings are consistent with previous studies. Zhong et al. (2012) noted that changes to floral color in *P. lactiflora* were related to the composition of pigments and the reduction in anthocyanins contributed to an increase in the L^* value and a decrease in the a^* value during the flowering period. Yang et al. (2015) investigated flower color change in two tree peony cultivars, 'Jinyi Hualian' and 'Xiaguang', and their results indicated that a sharp decrease in anthocyanins during the flowering period could be the main contributing factor for the change in color from red to orange and yellow.

In the flavonoid biosynthetic pathway, *CHS* is the first committed enzyme which can catalyze the synthesis of tetrahydroxy-chalcone from one molecule of 4-coumaroyl-CoA with three molecules of malonyl-CoA. *CHI* catalyzes the conversion of tetrahydroxy-chalcone into naringenin which is then converted into dihydroflavonols by *F3H* and *F3'H* and *F3'5'H*. Dihydroflavonols are then converted into colorless leucoanthocyanidins by the action of *DFR* or into yellow-colored flavones/flavonols by the action of *FLS*. Under the action of *ANS*, colorless leucoanthocyanidins are converted into corresponding colored anthocyanidins which are eventually converted into anthocyanins under the catalysis of *UFGT* (Winkel-Shirley, 2001; Tanaka, 2008). In the present study, we carried out a transcriptome analysis of 'Coral Sunset' at four stages (S1, S3, S5 and S7), and eight functional genes that were significantly differentially expressed in these stages were identified. The significantly high expression level of these functional genes during S1 contributed to the accumulation of anthocyanins during early stages and the sharply decreased expression level of these genes after S2 resulted in significant reduction of anthocyanin during later developmental stages, especially anthocyanins. Our results are consistent with previous studies. For example, Zhao et al. (2014) found that the lower expression of *PlPAL*, *PlFLS*, *PlDFR*, *PlANS*, *Pl3GT* and *Pl5GT* in the inner petals of *P. lactiflora* inhibited anthocyanin biosynthesis and resulted in the formation of yellow.

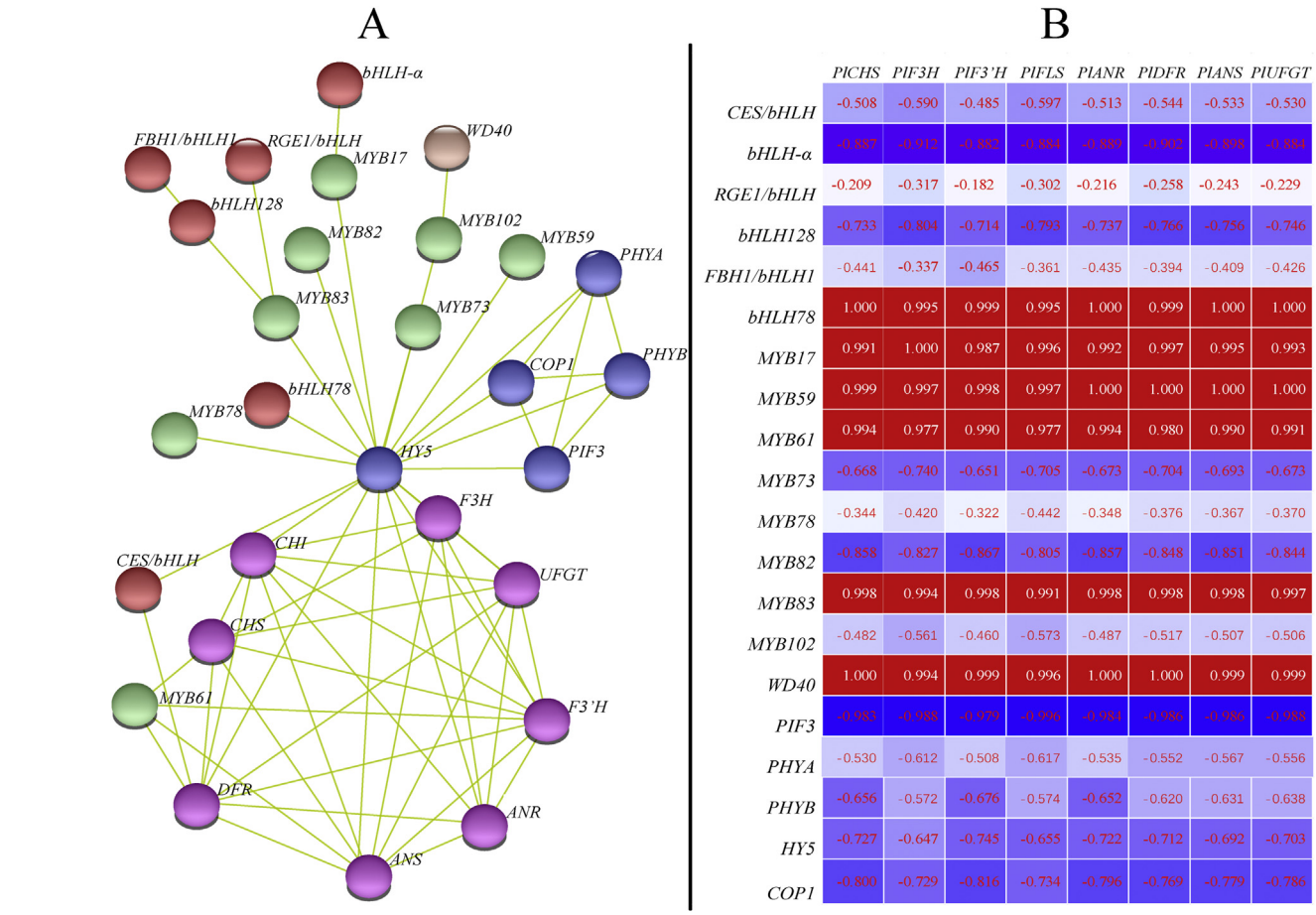

Fig. 7. A: Protein-protein interaction network of putative genes related to flavonoid biosynthesis; B: Co-expression of putative genes related to flavonoid biosynthesis.

Table 6
FPKM of transcription factors related to anthocyanin biosynthesis in petals of peony 'Coral Sunset' during different stages of flowering.

Gene name	#ID	Expression profile (FPKM)			
		S1	S3	S5	S7
MYB17	c106995.graph_c0	47.37	6.85	1.11	0.04
MYB59	c105957.graph_c0	63.89	2.93	1.15	0.31
MYB61	c102108.graph_c0	8.75	0	0.3	1.07
MYB73	c109598.graph_c0	1.12	5.89	33.51	28.99
MYB78	c104223.graph_c0	0.05	0	0.32	8.85
MYB82	c103958.graph_c0	4.28	27.33	32.29	17.02
MYB83	c108443.graph_c0	2.91	0.18	0	0.17
MYB102	c110511.graph_c0	0.09	2.71	8.91	35.16
CESTA/bHLH	c102820.graph_c0	0	5.06	25.54	77.86
bHLH-α	c105117.graph_c1	1.24	19.17	35.16	25.25
RGE1/bHLH	c108289.graph_c0	2.97	0.72	4.46	7.07
bHLH128	c108774.graph_c0	0.99	4.99	12	16.46
FBH1/Bhlh1	c118684.graph_c3	0	117.7	29.68	0.09
bHLH78	c80363.graph_c0	9.93	0.1	0	0
WD40	c110610.graph_c0	13.6	0.67	0.77	0.47
PIF3	c116287.graph_c0	6.87	56.12	53.64	64.75
PHYA	c116850.graph_c3	4.72	5.03	6.05	8.43
PHYB	c116870.graph_c0	23.63	37.55	32.78	25.78
HY5	c118268.graph_c2	20.59	74.31	40.1	15.66
COP1	c110069.graph_c1	4.16	8.21	6.97	5.65

The expression of structural genes in anthocyanin biosynthesis is regulated by three TFs, *MYB*, *bHLH* and *WD40*, which can form a MYB-bHLH-WD40 (MBW) transcriptional activation complex (Tanaka, 2008; Shi et al., 2018). In this study, three *bHLH*, five *MYB* and one *WD40* TFs were identified and co-expression analysis showed that these TFs

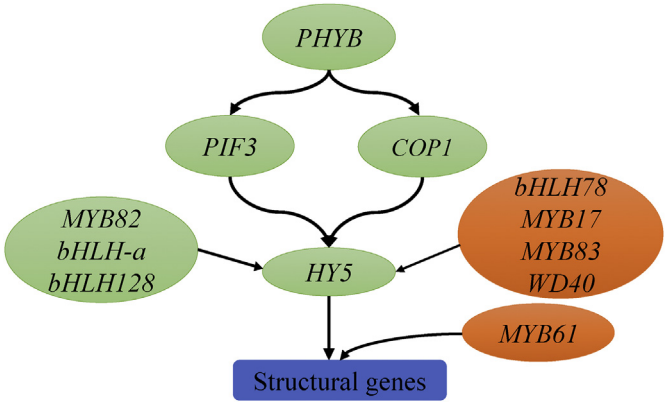

Fig. 8. Proposed regulatory model between TFs and structural genes in petals of peony 'Coral Sunset' during seven stages of flowering.

showed a close correlation with the functional genes. Protein-protein interaction showed that these TFs were connected with functional genes through HY5, which acts downstream of the light receptor network and directly affects transcription of light-induced genes. This indicates that the expression of functional genes and the reduction of anthocyanins might be related to light. Many researches have showed that the transcription factors HY5, MYB, bHLH and WD40 COP1, PIF3 and PHYB are related to anthocyanin biosynthesis. Liu et al. (2018) found that the expression of CHS and DFR genes in tomato could be regulated by transcription factor HY5, which could response to light. Functional testing proved the *MdFLS* promoter of apple could be activated by HY5 of which transcription were down-regulated under reduced UV light

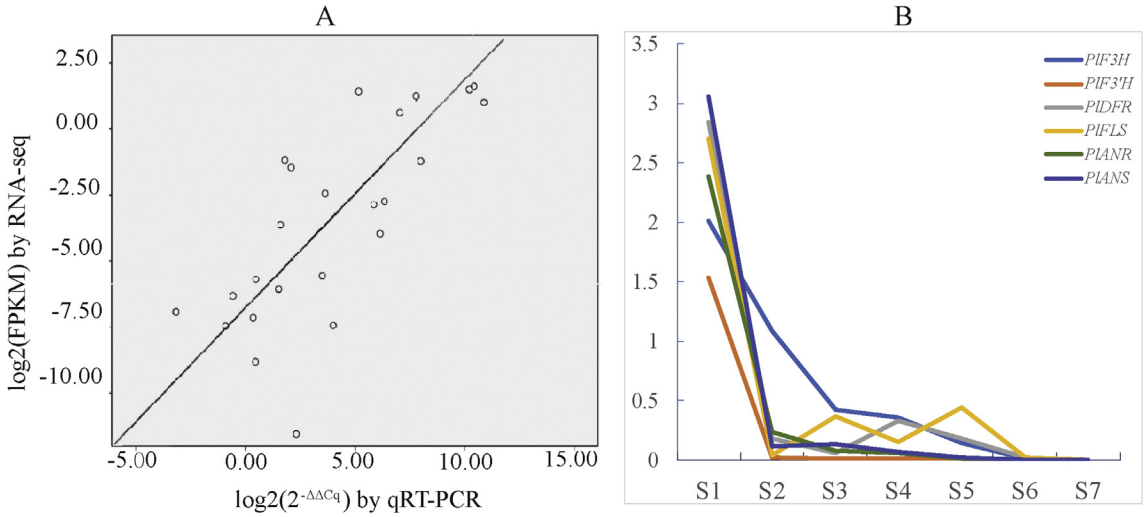

Fig. 9. qRT-PCR validation of anthocyanin biosynthesis-related genes in petals of peony 'Coral Sunset' during seven stages of flowering. A: Correlation of the expression of structural genes by qRT-PCR and RNA-seq. B: Expression patterns of six structural genes during seven stages.

level (Henry-Kirk et al., 2018). Tao et al. (2018) revealed that the conserved blue light signal transduction module CRY-COP1-HY5 contributed to the anthocyanin biosynthesis under blue light in red pear. Maier et al. (2013) found that the light response element COP1 could interact with the MYB transcription factors PAP1 and PAP2 and affect the biosynthesis of anthocyanins at transcriptional and post-transcriptional levels.

In conclusion, the high expression of eight structural genes (*PlCHS*, *PlF3H*, *PlF3'H*, *PlFLS*, *PlDRF*, *PlANR*, *PlANS* and *PlUFGT*) during S1 contributed to the accumulation of anthocyanins. The extremely low expression level of these structural genes during other stages resulted in a significant reduction of anthocyanins, which caused petal color to change from coral to pink to yellow. TFs *bHLH78*, *bHLH-a*, *bHLH128*, *MYB17*, *MYB59*, *MYB73*, *MYB82*, *MYB61*, *WD40*, *PIF3*, *PHYB*, *HY5* and *COP1* might work together to regulate the expression of these structural genes.

Author contributions

Conceived and designed the experiments: Xiaonan Yu.
Performed the experiments: Yujiao Wang.
Analyzed the data: Yujiao Wang.
Wrote the paper: Liping Guo, Yujiao Wang.
Reviewed and edited the paper: Liping Guo, Jaime A. Teixeira da Silva, Xiaonan Yu, Yongming Fan.

Conflicts of interest

The authors hereby declare no conflicts of interest.

Acknowledgements

This work was financially supported by the National Natural Science Foundation of China (31400591).

Appendix A. Supplementary data

Supplementary data to this article can be found online at https://doi.org/10.1016/j.plaphy.2019.02.025.

References

Anders, S., Huber, W., 2010. Differential expression analysis for sequence count data. Genome Biol. 11, R106.
Cao, Y.T., 2012. Cloning the Full Length cDNA of Anthocyanins Biosynthesis Key Genes and *CHS* Gene Promote from *Brunfelsia Acuminata* Flowers. Fuzhou: Fujian Agriculture and Forestry University (in Chinese).
Constant, H.L., Slowing, K., Graham, J.G., Pezzuto, J.M., Cordell, G.A., Beecher, C.W.W., 2015. A general method for the dereplication of flavonoid glycosides utilizing high performance liquid chromatography/mass spectrometric analysis. Phytochem. Anal. 8 (4), 176–180.
Deng, J., Fu, Z.Y., Chen, S., Njeri, R., Wang, K., Li, T., Yang, P.F., 2015. Proteomic and epigenetic analyses of lotus (*Nelumbo nucifera*) petals between red and white cultivars. Plant Cell Physiol. 56 (8), 1546–1555.
Fu, L., Li, H., Li, L., Yu, H., Wang, L., 2013. Reason of flower color change in *Lonicera japonica. 2013*. Sci. Silvae Sin. 49 (10), 155–161 (in Chinese).
Grabherr, M.G., Haas, B.J., Yassour, M., Levin, J.Z., Thompson, D.A., Amit, I., Adiconis, X., Fan, L., Raychowdhury, R., Zeng, Q., Chen, Z., Mauceli, E., Hacohen, N., Gnirke, A., Rhind, N., di Palma, F., Birren, B.W., Nusbaum, C., Lindblad-Toh, K., Friedman, N., Regev, A., 2011. Full-Length transcriptome assembly from RNA-seq data without a reference genome. Nat. Biotechnol. 29 (7), 644–652.
Henry-Kirk, R.A., Plunkett, B., Hall, M., Mcghie, T., Allan, A.C., Wargent, J.J., Espley, R., 2018. Solar UV light regulates flavonoid metabolism in apple (*malus x domestica)*. Plant Cell Environ. 41 (3), 1–14.
Jia, N., Shu, Q., Wang, L., Du, H., Xu, Y., Liu, Z., 2008. Analysis of petal anthocyanins to investigate coloration mechanism in herbaceous peony cultivars. Sci. Hortic. 117 (2), 167–173.
Liu, C., Chi, C., Jin, L., Zhu, J., Yu, J., Zhou, Y., 2018. The bZIP transcription factor HY5 mediates cry1a-induced anthocyanin biosynthesis in tomato. Plant Cell Environ. 41 (8), 1762.
Liu, L., Zhang, L., Wang, S., Niu, X., 2016. Analysis of anthocyanins and flavonols in the petals of 10 Rhododendron species from the sygera mountains in southeast tibet. Plant Physiol. Biochem. 104, 250–256.
Maier, A., Schrader, A., Kokkelink, L., Falke, C., Welter, B., Iniesto, E., Rubio, V., Uhrig, J.F., Hülskamp, M., Hoecker, U., 2013. Light and the E3 ubiquitin ligase COP1/SPA control the protein stability of the MYB transcription factors PAP1 and PAP2 involved in anthocyanin accumulation in Arabidopsis. Plant J. 74, 638–651.
Mortazavi, A., Williams, B.A., Mccue, K., Schaeffer, L., Wold, B., 2008. Mapping and quantifying mammalian transcriptomes by RNA-Seq. Nat. Methods 5, 621–628.
Shi, L., Chen, X., Chen, W., Zheng, Y., Yang, Z., 2018. Comparative transcriptomic analysis of white and red Chinese bayberry (*Myrica rubra*) fruits reveals flavonoid biosynthesis regulation. Sci. Hortic. 235, 9–20.
Tanaka, Y., Brugliera, F., Chandler, S., 2009. Recent progress in flower color modification by biotechnology. Int. J. Mol. Sci. 10, 5350–5369.
Tao, R., Bai, S., Ni, J., Yang, Q., Zhao, Y., Teng, Y., 2018. The blue light signal transduction pathway is involved in anthocyanin accumulation in 'red zaosu' pear. Planta 248 (1), 37–48.
Teppabut, Y., Oyama, K., Kondo, T., Yoshida, K., 2018. Change of petals' color and chemical components in *Oenothera* flowers during senescence. Molecules 1698.
Wang, J., Zhang, Z., 2005. Herbaceous Peonies of China. China Forestry Publishing House, pp. pp3 (in Chinese).
Winkel-Shirley, B., 2001. Flavonoid biosynthesis. a colorful model for genetics, biochemistry, cell biology, and biotechnology. Plant Physiol. 126 (2), 485–493.
Wu, Q., Li, P., Zhang, H., Feng, C., Li, S., Yin, D., Tian, J., Xu, W., Wang, L., 2018. Relationship between the flavonoid composition and flower colour variation in *Victoria*. Plant Biol. 20, 674–681.
Xue, L., Wang, Z., Zhang, W., Li, Y., Wang, J., Lei, J., 2016. Flower pigment inheritance and anthocyanin characterization of hybrids from pink-flowered and white-flowered strawberry. Sci. Hortic. 200, 143–150.
Yang, Q., Yuan, H.H., Sun, X.B., 2015. Preliminary studies on the changes of flower color during the flowering period in two tree peony cultivars. Acta Hortic. Sin. 42 (5),

930–938.
Yu, X., Song, H., Zheng, L., 2010. Brief introduction of breeding and horticulture utilization of ornamental herbaceous peony at abroad. Journal of Hunan Agricultural University (Natural Sciences) 36 (2), 159–162 (in Chinese).
Zhao, D., Tao, J., Han, C., 2012. Flower color diversity revealed by differential expression of flavonoid biosynthetic genes and flavonoid accumulation in herbaceous peony (*Paeonia lactiflora* Pall.). Mol. Biol. Rep. 39 (12), 11263–11275.
Zhao, D.Q., Wei, M.R., Liu, D., Tao, J., 2016. Anatomical and biochemical analysis reveal the role of anthocyanins in flower coloration of herbaceous peony. Plant Physiol. Biochem. 102, 97–106.
Zhao, D., Jiang, Y., Ning, C., et alMeng, J., Lin, S., Ding, W., Tao, J., 2014. Transcriptome sequencing of a chimaera reveals coordinated expression of anthocyanin biosynthetic genes mediating yellow formation in herbaceous peony (*Paeonia lactiflora* Pall.). BMC Genomics 15 (1), 689–706.
Zhao, D., Wei, M., Min, S., Hao, Z., Tao, J., 2017. Identification and comparative profiling of miRNAs in herbaceous peony (*Paeonia lactiflora* Pall.) with red/yellow bicoloured flowers. Sci. Rep. 7, 44926.
Zhong, P.X., Wang, L.S., Li, S.S., Xu, Y.J., Zhu, M.L., 2012. The changes of floral color and pigments composition during the flowering period in *Paeonia lactiflora* Pall. Acta Hortic. Sin. 39 (11), 2271–2282.
Zipor, G., Duarte, P., Carqueijeiro, I.M., Shahar, L., Ovadia, R., Teper-bamnolker, P., Eshel, D., Levin, Y., Faigenboim, A., Sottomayor, M., Oren-Shamir, M., 2015. In planta anthocyanin degradation by a vacuolar class III peroxidase in Brunfelsia calycina flowers. 2015. New Phytol. 205 (2), 653–665.